ELECTRONIC SUPPLEMENTARY INFORMATION (ESI)

Speciation in human blood of Metvan, a vanadium based potential anti-tumor drug

Daniele Sanna,[a] Valeria Ugone,[b] Giovanni Micera,[b] Péter Buglyó,[c] Linda Bíró,[c]
Eugenio Garribba,*[b]

[a] *Istituto CNR di Chimica Biomolecolare, Trav. La Crucca 3, I-07040 Sassari, Italy*

[b] *Dipartimento di Chimica e Farmacia, Università di Sassari, Via Vienna 2, I-07100 Sassari, Italy. E-mail: garribba@uniss.it; Tel: +39 079 229487.*

[c] *Department of Inorganic and Analytical Chemistry, University of Debrecen, H-4032 Debrecen, Egyetem tér 1, Hungary*

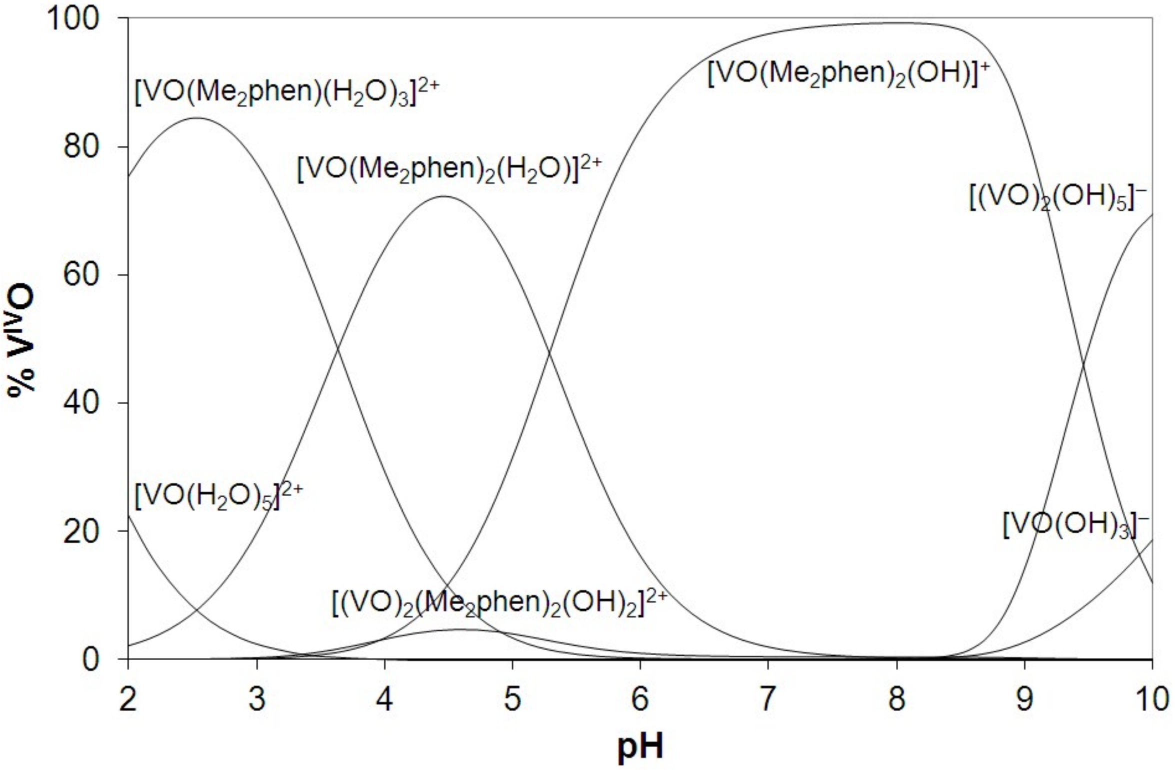

Figure S1. Concentration distribution curves of the species formed in the system $V^{IV}O^{2+}$/Me_2phen with a molar ratio of 1/5 and V concentration of 1.0 × 10^{-3} M.

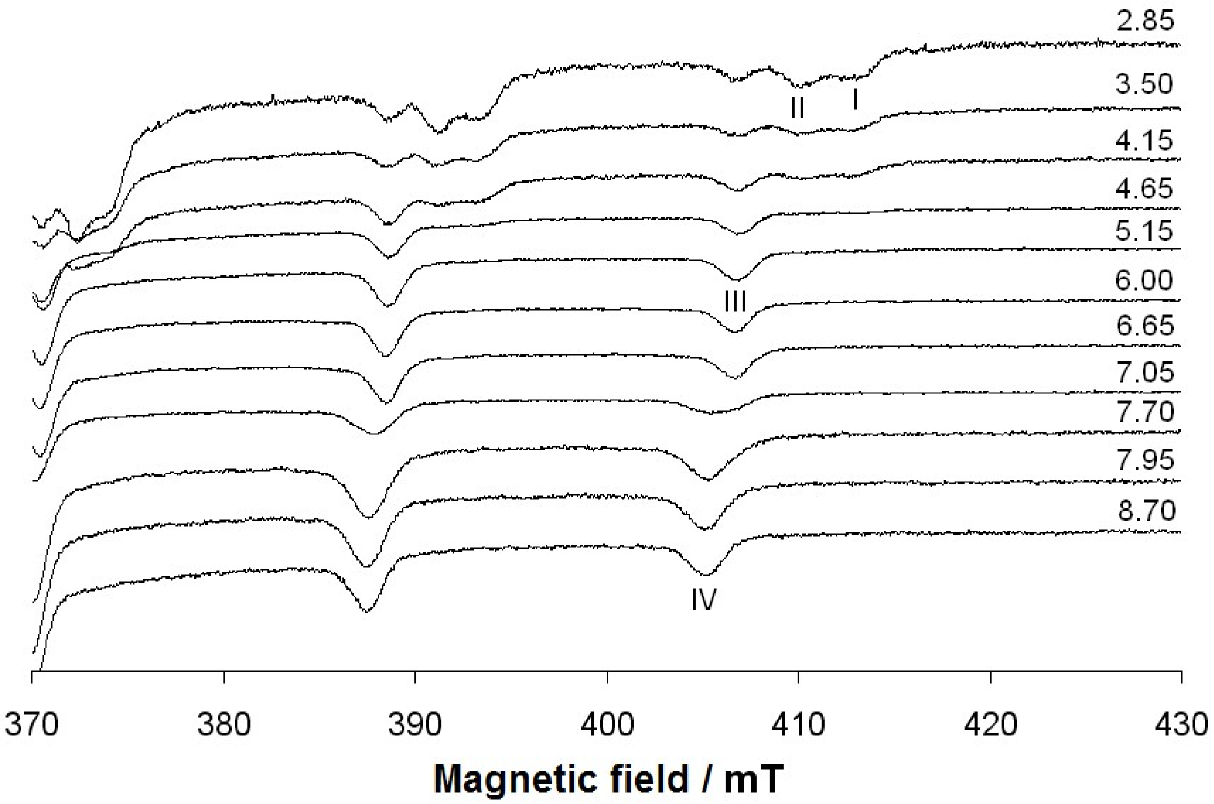

Figure S2. High field region of the X-band anisotropic EPR spectra recorded at 120 K as a function of pH in the system $V^{IV}O^{2+}$/Me_2phen with a molar ratio of 1/5 and V concentration of 1.0 × 10^{-3} M. The M_I = 7/2 resonance of [VO(Me_2phen)(H_2O)$_3$]$^{2+}$ (equatorial-equatorial coordination) is indicated with **I**, of [VO(Me_2phen)(H_2O)$_3$]$^{2+}$ (equatorial-axial coordination) with **II**, of *cis*-[VO(Me_2phen)$_2$(H_2O)]$^{2+}$ with **III**, and of *cis*-[VO(Me_2phen)$_2$(OH)]$^{+}$ with **IV**.

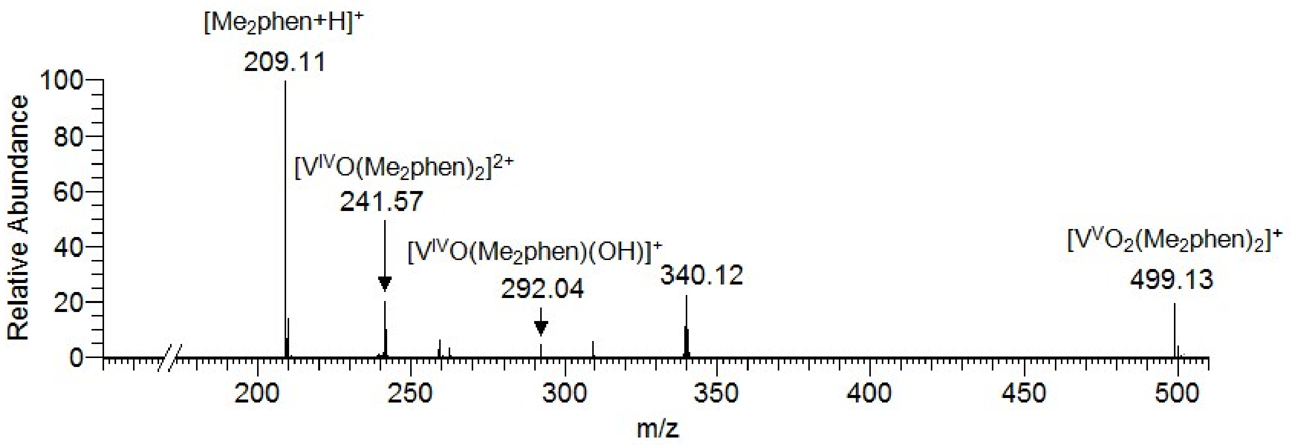

Figure S3. ESI mass spectrum recorded in the positive mode at pH 4.80 in ultrapure LC-MS water in the system $V^{IV}O^{2+}$/Me_2phen with a molar ratio of 1/2 and V concentration of 1.0×10^{-5} M.

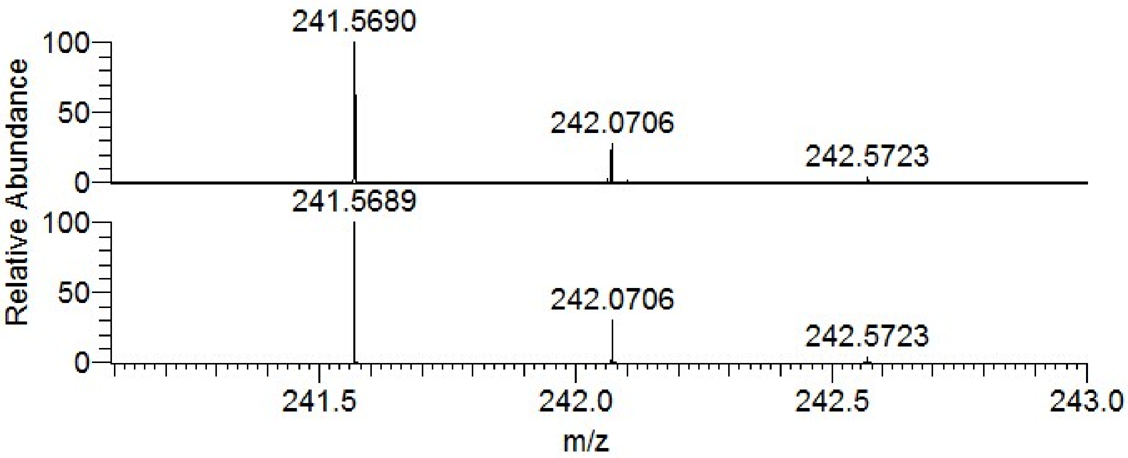

Figure S4. Experimental (a) and calculated (b) isotopic pattern for the peak of $[V^{IV}O(Me_2phen)_2]^{2+}$ revealed at m/z = 241.57 in the positive ESI-MS spectrum recorded on the system $V^{IV}O^{2+}/Me_2phen$ (ultrapure LC-MS water, pH 4.80, molar ratio 1/2, V concentration 1.0×10^{-5} M).

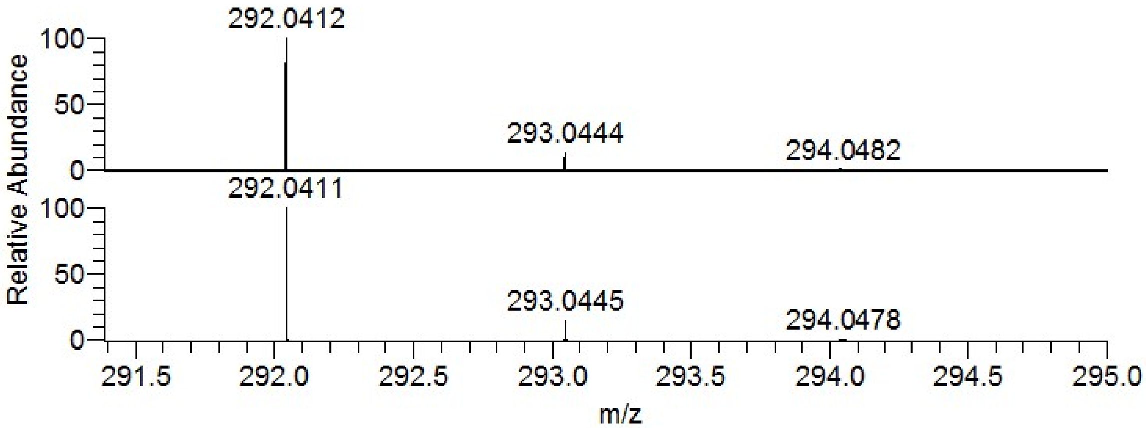

Figure S5. Experimental (a) and calculated (b) isotopic pattern for the peak of $[V^{IV}O(Me_2phen)(OH)]^+$, revealed at m/z = 292.04 in the positive ESI-MS spectrum recorded on the system $V^{IV}O^{2+}/Me_2phen$ (ultrapure LC-MS water, pH 4.80, molar ratio 1/2, V concentration 1.0×10^{-5} M).

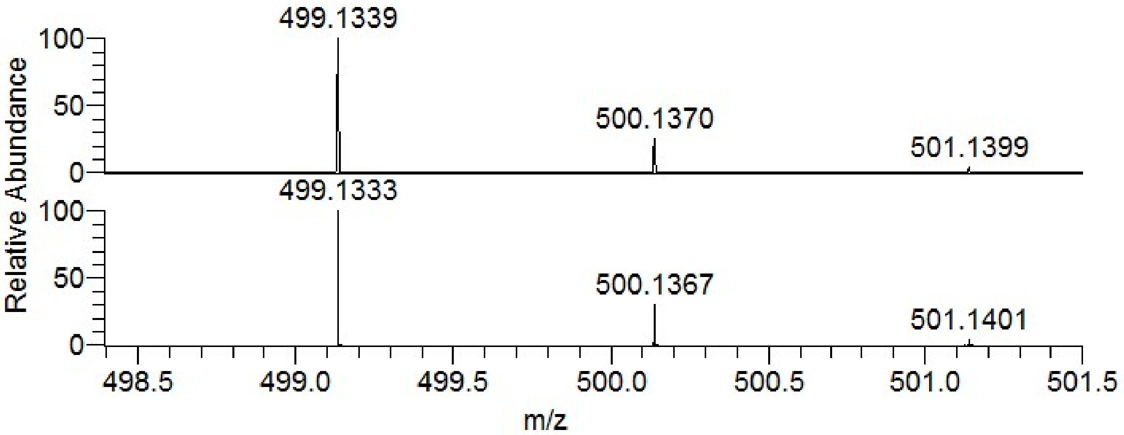

Figure S6. Experimental (a) and calculated (b) isotopic pattern for the peak of $[V^{V}O_2(Me_2phen)_2]^+$ revealed at m/z = 499.13 in the positive ESI-MS spectrum recorded on the system $V^{IV}O^{2+}/Me_2phen$ (ultrapure LC-MS water, pH 4.80, molar ratio 1/2, V concentration 1.0×10^{-5} M).

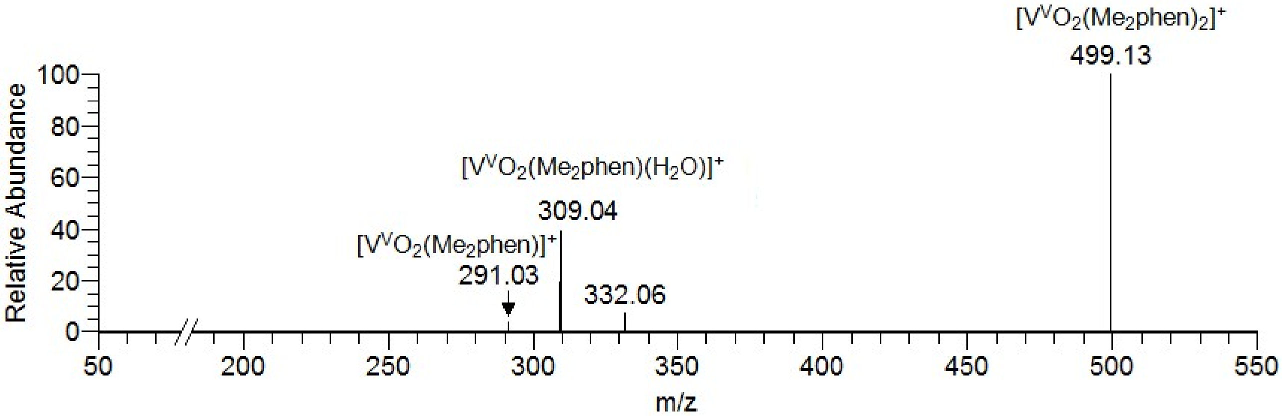

Figure S7. ESI-MS/MS spectrum of the fragment $[V^VO_2(Me_2phen)_2]^+$ recorded on the system $V^{IV}O^{2+}/Me_2phen$ (positive ion mode, m/z = 499.5 ± 1.0, ultrapure LC-MS water, pH 4.80, molar ratio 1/2, V concentration 1.0×10^{-5} M).

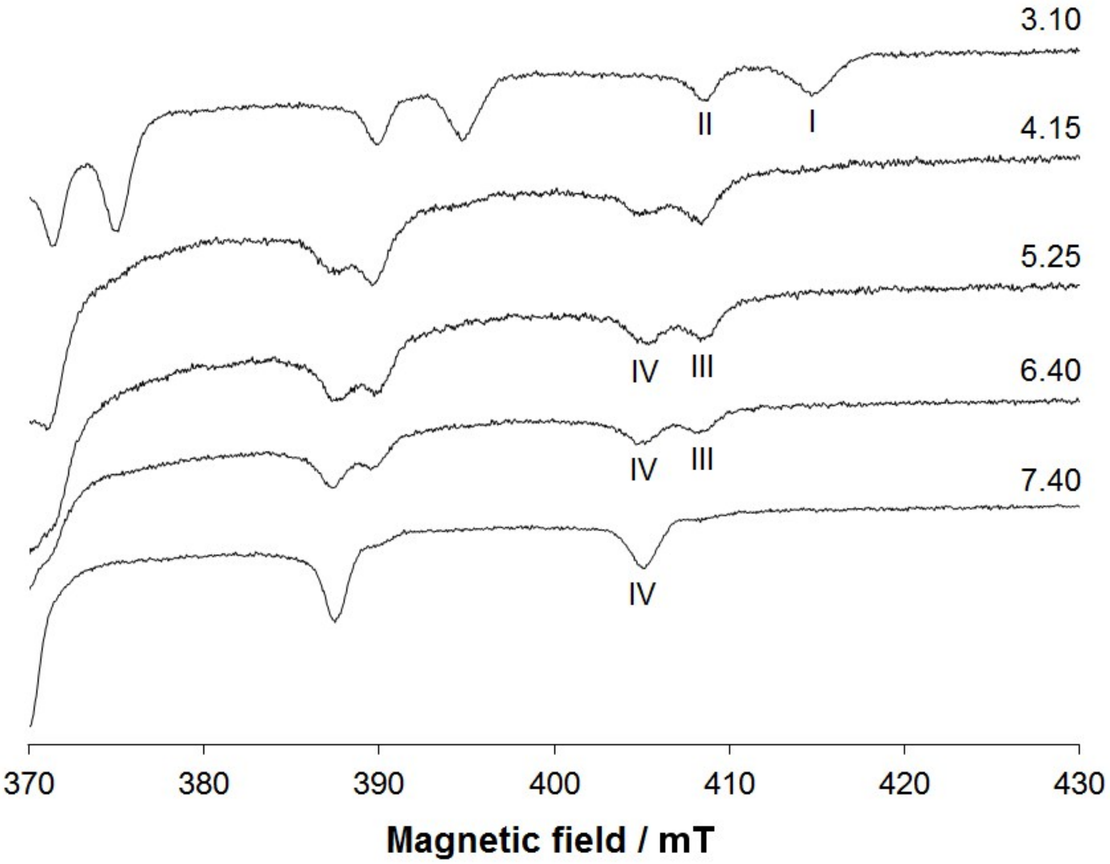

Figure S8. High field region of the X-band anisotropic EPR spectra recorded at 120 K as a function of pH in the system $V^{IV}O^{2+}$/Me_2phen/H_3citr with a molar ratio of 1/2/2 and V concentration of 1.0×10^{-3} M. The M_I = 7/2 resonance of $[VO(citrH)(H_2O)_2]^{2+}$ is indicated with **I**, of $[VO(Me_2phen)(citrH)]$ with **II**, of $[VO(Me_2phen)(citr)]^-$ with **III** and of $[VO(Me_2phen)(citrH_{-1})]^{2-}$ with **IV**.

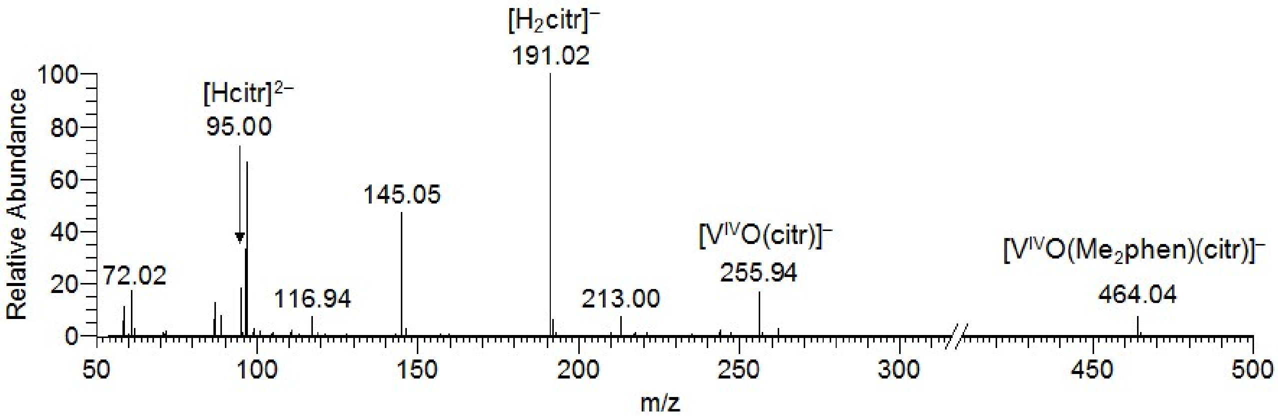

Figure S9. ESI mass spectrum recorded in the negative mode at pH 4.90 in ultrapure LC-MS water in the system $V^{IV}O^{2+}$/Me_2phen/H_3citr with a molar ratio of 1/2/2 and V concentration of 2.5×10^{-6} M.

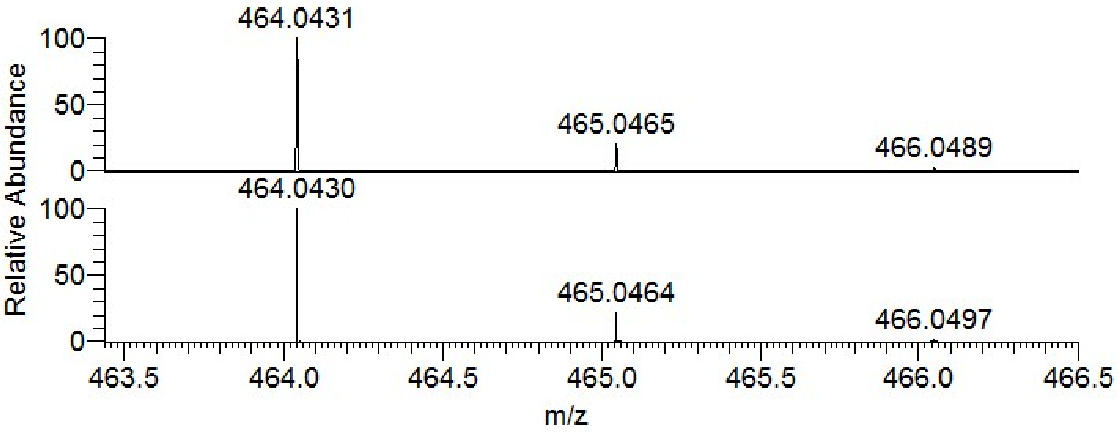

Figure S10. Experimental (a) and calculated (b) isotopic pattern for the peak of [$V^{IV}O(Me_2phen)(citr)]^-$ revealed at m/z = 464.03 in the negative ESI-MS spectrum recorded on the system $V^{IV}O^{2+}/Me_2phen/H_3citr$ (ultrapure LC-MS water, pH 4.90, molar ratio 1/2/2, V concentration 2.5×10^{-6} M).

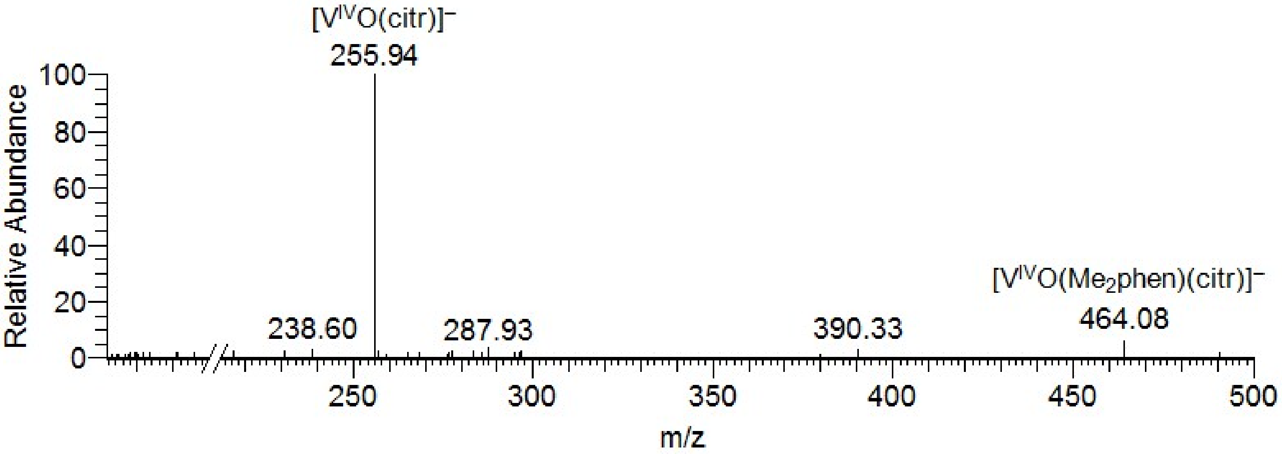

Figure S11. ESI-MS/MS spectrum of the fragment [$V^{IV}O(Me_2phen)(citr)]^-$ recorded on the system $V^{IV}O^{2+}/Me_2phen/H_3citr$ (negative ion mode, m/z = 464.0 ± 1.0, ultrapure LC-MS water, pH 4.90, molar ratio 1/2/2, V concentration 2.5×10^{-6} M).

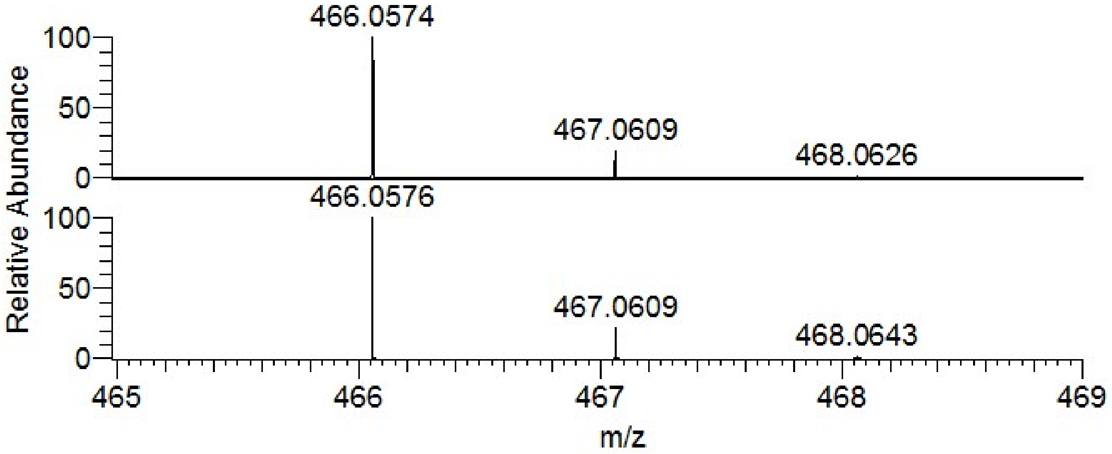

Figure S12. Experimental (a) and calculated (b) isotopic pattern for the peak of [$V^{IV}O(Me_2phen)(citr)+2H]^+$ revealed at m/z = 466.06 in the positive ESI-MS spectrum recorded on the system $V^{IV}O^{2+}/Me_2phen/H_3citr$ (ultrapure LC-MS water, pH 4.90, molar ratio 1/2/2, V concentration 2.5×10^{-6} M).

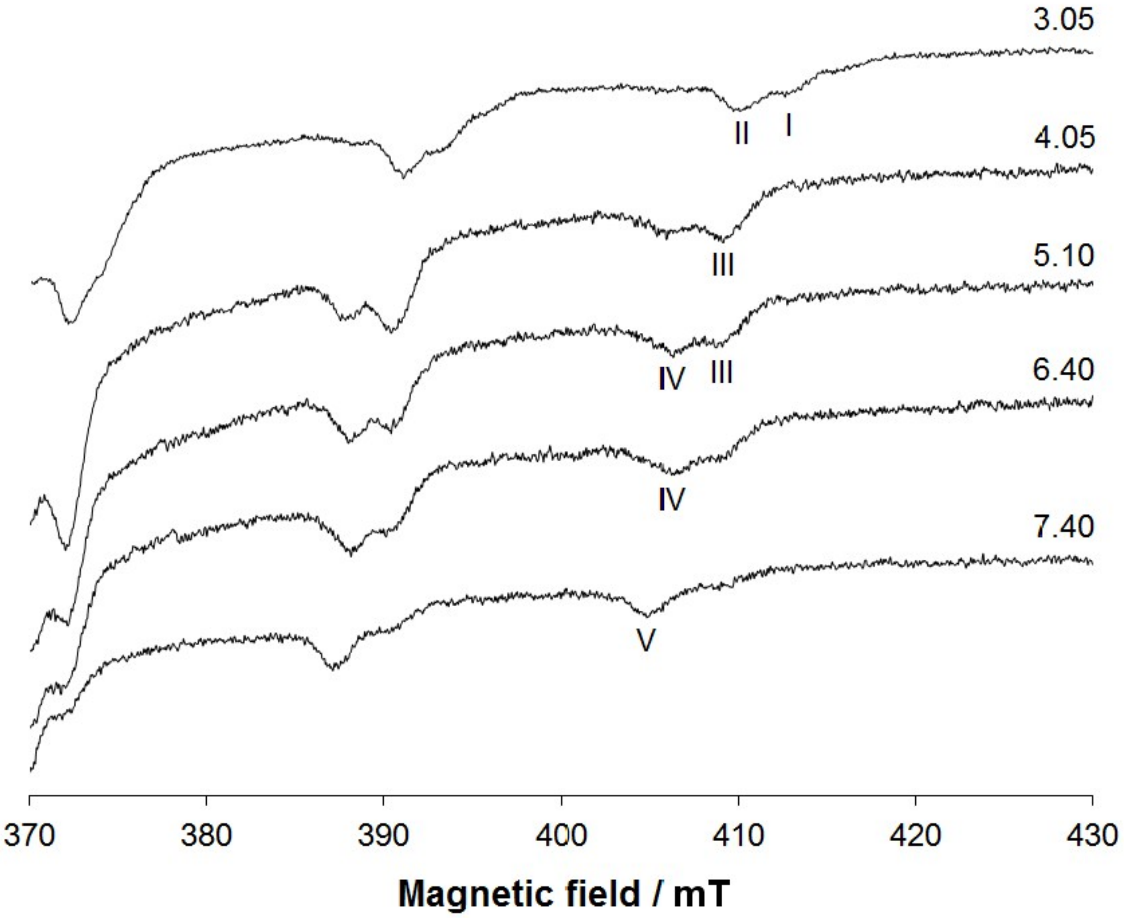

Figure S13. High field region of the X-band anisotropic EPR spectra recorded at 120 K as a function of pH in the system $V^{IV}O^{2+}$/Me_2phen/Hlact with a molar ratio of 1/2/4 and V concentration of 1.0 × 10^{-3} M. The $M_I = 7/2$ resonance of $[VO(Me_2phen)(H_2O)_3]^{2+}$ (equatorial-equatorial coordination) is indicated with **I**, of $[VO(Me_2phen)(H_2O)_3]^{2+}$ (equatorial-axial coordination) with **II**, of $[VO(Me_2phen)(lact)(H_2O)]^{+}$ with **III**, of *cis*-$[VO(Me_2phen)_2(H_2O)]^{2+}$ with **IV** and of *cis*-$[VO(Me_2phen)_2(OH)]^{+}$ with **V**.

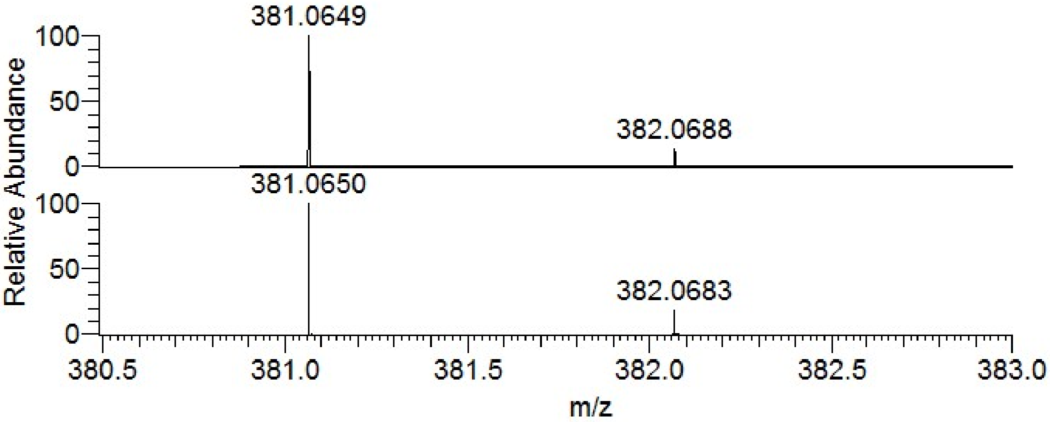

Figure S14. Experimental (a) and calculated (b) isotopic pattern for the peak of $[V^{V}O_2(Me_2phen)(lact)+H]^+$ revealed at m/z = 381.06 in the positive ESI-MS spectrum of the system $V^{IV}O^{2+}/Me_2phen/Hlact$ in ultrapure LC-MS water (pH 3.80, molar ratio of 1/2/4, V concentration of 5.0×10^{-6} M).

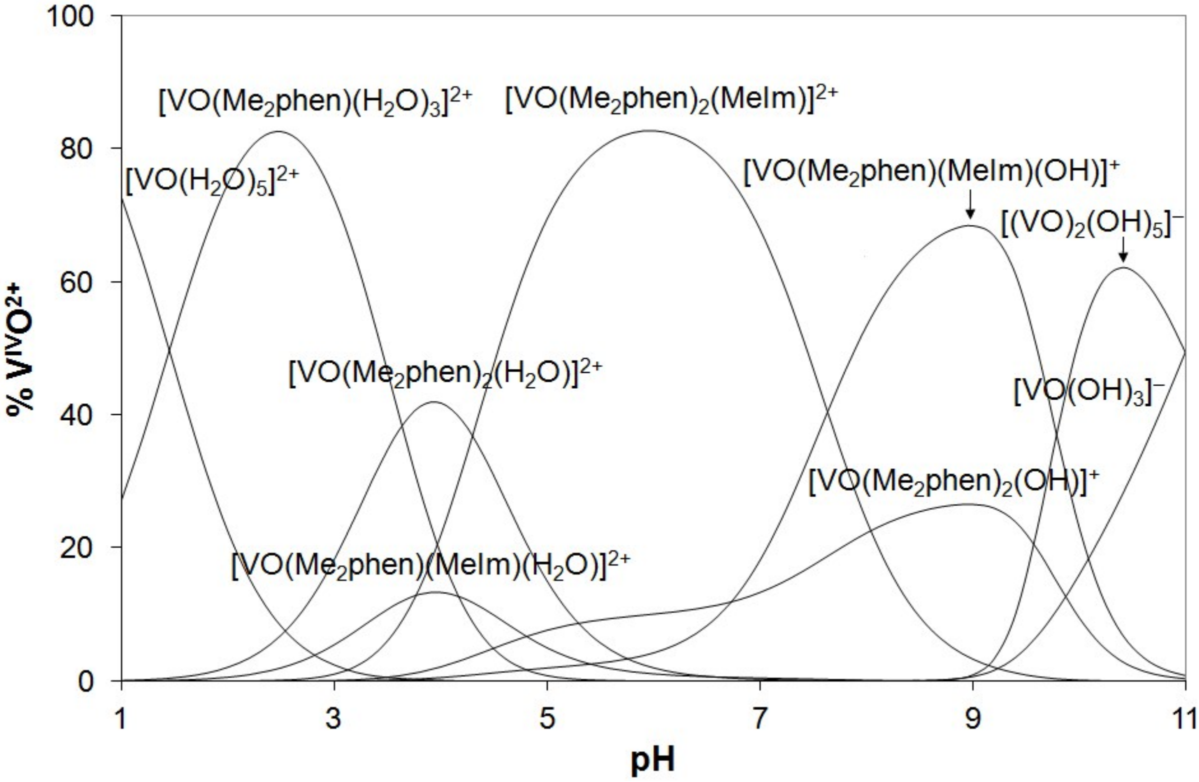

Figure S15. Concentration distribution curves of the species formed in the system $V^{IV}O^{2+}$/Me_2phen/MeIm with a molar ratio of 1/5/4 and V concentration of 1.0×10^{-3} M.

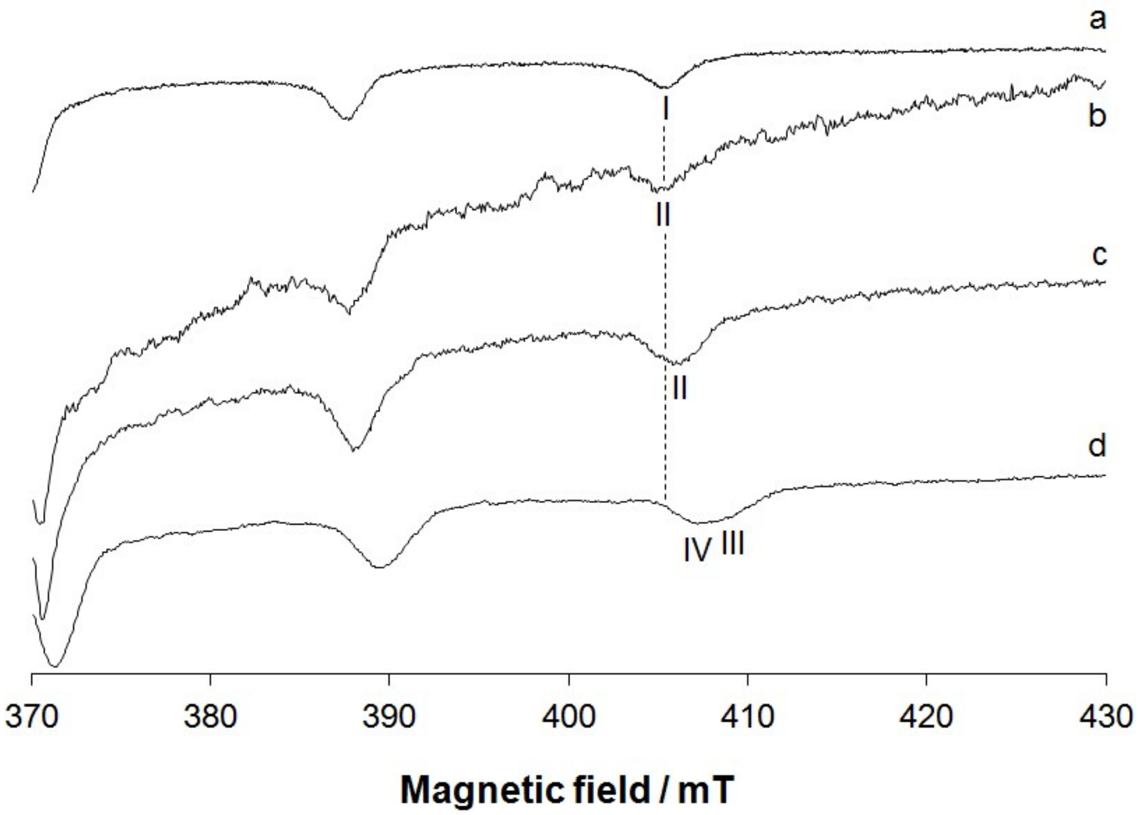

Figure S16. High field region of the X-band anisotropic EPR spectra recorded at 120 K at pH 7.4 in the system containing: a) $V^{IV}O^{2+}$/Me_2phen/MeIm 1/2/4 ($V^{IV}O^{2+}$ 1.0 × 10^{-3} M); b) $V^{IV}O^{2+}$/Me_2phen/Hb 2/4/1 ($V^{IV}O^{2+}$ 6.2 × 10^{-4} M); c) $V^{IV}O^{2+}$/Me_2phen/Hb 2/10/1 ($V^{IV}O^{2+}$ 6.2 × 10^{-4} M) and d) $V^{IV}O^{2+}$/Hb 2/1 ($V^{IV}O^{2+}$ 6.2 ×10^{-4} M). The M_I = 7/2 resonance of the species $[VO(Me_2phen)(MeIm)(OH)]^+$ and *cis*-$[VO(Me_2phen)_2(MeIm)]^{2+}$ is indicated with **I**, of VO−Me_2phen−Hb with **II** and of the sites β and γ of Hb ($(VO)Hb^{\beta}$ and $(VO)Hb^{\gamma}$) with **III** and **IV**. The M_I = 7/2 resonance of VO−Me_2phen−Hb is also denoted by the dotted line.